Bioresource Technology 451 (2026) 134544

Contents lists available at ScienceDirect

Bioresource Technology

journal homepage: www.elsevier.com/locate/biortech

Adhesion and binding properties of extracellular polymeric substances (EPS) extracted from activated sludge☆

Ji Li *, Jeenah Hermelijn, Mark C.M. van Loosdrecht, Yuemei Lin

Department of Biotechnology, Delft University of Technology, van der Maasweg 9, 2629 HZ Delft, the Netherlands

HIGHLIGHTS

- EPS exhibited strong adhesion to both hydrophilic and hydrophobic surfaces.
- EPS showed high microbead binding capacities of 2.0–6.0 mg beads per mg EPS.
- EPS effectively delivered microbeads onto both surface types.
- EPS adhesion performance was significantly influenced by pH and total solids (TS).
- EPS from activated sludge demonstrated potential as natural adhesives and binders.

GRAPHICAL ABSTRACT

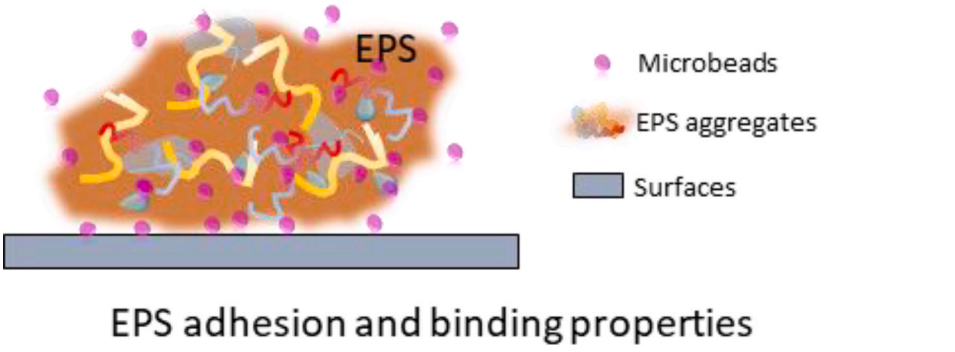

ARTICLE INFO

Keywords:
Extracellular polymeric substances (EPS)
Activated sludge
Surface adhesion
Hydrophilic and hydrophobic surfaces
Adsorption isotherm model
Microbead binding

ABSTRACT

Extracellular polymeric substances (EPS) harvested from biological sludge can be utilized as high-value biomaterials. This study investigated the adhesion and binding properties of activated sludge EPS on hydrophilic and hydrophobic surfaces under varying pH and total solids (TS) levels. At a 2.5% TS content, lower pH was able to enhance adhesion performance on both surface types, yielding capacities of 1000–2500 mg/m^2 and 500–1500 mg/m^2 for hydrophilic and hydrophobic surfaces, respectively. Increased TS further promoted surface adhesion, however saturation occurred at approximately 2500 mg/m^2 on hydrophilic surfaces at 5.3% TS, whereas adhesion continued to increase on hydrophobic surfaces. Adsorption isotherm model simulations suggested that EPS-surface interactions were governed by distinct adsorption mechanisms. The distribution of functional groups and the structural arrangement of EPS aggregates, modulated by pH and TS, appeared to regulate these interfacial interactions. Additionally, EPS exhibited strong microbead binding capacities ranging from 2.0–6.0 mg beads per mg EPS, facilitating effective attachment of microbeads to both surface morphologies. These findings proved the potential of EPS as versatile, sustainable, bio-based adhesives and binders with broad applicability.

☆ This article is part of a special issue entitled: 'IWA ecoSTP2025' published in Bioresource Technology.

* Corresponding author.
E-mail address: J.Li-24@tudelft.nl (J. Li).

https://doi.org/10.1016/j.biortech.2026.134544
Received 5 February 2026; Received in revised form 31 March 2026; Accepted 31 March 2026
Available online 1 April 2026

1. Introduction

In water biofilms, extracellular polymeric substances (EPS) are secreted by microorganisms and act as both the structural and functional matrix of the biofilm (Flemming and Wingender, 2010; Wang et al., 2021). Within EPS, various components including polysaccharides, proteins, lipids, nucleic acids, and so on, have been identified as dominant structural fractions. Owing to these diverse components and involved functional groups, EPS enveloped microbial cells and consequently modified their physiochemical characteristics, such as surface charge, hydrophobicity and polymeric properties. These alterations not only mediated cellular recognition but also facilitate initial cell adhesion and aggregation (Harimawan and Ting, 2016).

A functional definition of EPS was introduced in a glossary to the report of the Dahlem Workshop on Structure and Function of Biofilms in Berlin, 1988 (Characklis and Wilderer, 1989; Flemming et al., 2010); here, EPS were defined as "organic polymers of microbial origin which in biofilm systems are frequently responsible for immobilizing cells and other particulate materials together (cohesion) and to the substratum (adhesion)". This definition highlighted the characteristic role of EPS as a biological "glue" that stabilized microbial aggregates. Subsequent studies have experimentally verified the adhesion properties of EPS. For example, Zaidi et al. (2019) demonstrated that EPS-rich strains exhibited stronger adhesion to surfaces than EPS-deficient strains under comparable surface charge conditions. Similarly, Wang et al. (2021) isolated distinct EPS layers from granular sludge and confirmed that EPS enhanced cell adhesion and aggregates in the granulation by improving zeta potential and hydrophobicity.

Beyond their structural functions of adhesion within biofilms, extracted EPS (out of sludge) have also been shown to possess natural adhesive and cohesive capacities. Omoike et al. (2004) extracted EPS from both *Bacillus subtilis* (Gram-positive) and *Pseudomonas aeruginosa* (Gram-negative) and observed an energetically stable bond of EPS with the goethite (R-FeOOH) surface. Likewise, Zhu et al. (2009) isolated EPS from four bacterial strains and, through quartz crystal microbalance with dissipation (QCM-D) analysis, demonstrated that EPS deposition rates on silica surfaces were maximized under low ionic strength conditions in both NaCl and $CaCl_2$ solutions. Furthermore, Ou et al. (2020) compared EPS extracted from activated sludge interactions with different charged membranes and found that bound EPS exhibited higher affinity to membranes than dissolved EPS. More recently, Chen et al. (2024) extracted EPS from granular sludge and revealed that EPS could form stable adhesive layers between two glass slides, achieving shear strengths of 36–51 kPa without additional chemical pretreatment.

Collectively, these studies confirmed the adhesion nature of EPS. However, while most research has focused on EPS derived from pure cultures biomass or granular sludge, the adhesion properties of EPS from activated sludge are lack of knowledge. According to Li et al. (2021), EPS yield from activated sludge accounts for 9–19% of the total volatile solids, which is notably lower than that from granular sludge (around 19–30%)(Li et al., 2021, 2025). Nevertheless, the vast quantities of sewage sludge generated annually made activated sludge an abundant and reliable source for EPS recovery. For instance, sewage treatment plants were estimated to produce approximately 17 million tons of dry sludge per year in Europe (Bianchini et al., 2016), over 20 million tons in China in 2022 (Liu et al., 2025) and 7.9–7.1 million tons annually in the United States from 2010 to 2020 (Krause and Bronstein, 2024).

On the other hand, studies have already demonstrated that EPS extracted from activated sludge has wide-ranging applications, including wood adhesives, pollutant adsorption, flame retardancy, corrosion inhibition, hydrogel formation, and surface coatings. These applications are inherently linked to the adhesive and binding capabilities of EPS. For instance, when EPS is utilized as fillers or coatings for flame retardants, its adhesion to the substrate is as critical as the flame-retardant mechanism itself. Furthermore, in foliar spray applications, where nutrient absorption through leaves is often more efficient than root uptake, with adhesion and binding capacity, the usage of EPS could enhance the mixture with nutrients and improve leaf retention time, which would improve crop yield and quality under environmental stresses. Therefore, it is interesting to investigate whether EPS from activated sludge possess the adhesion nature and determine the specific conditions that optimize its performance.

To bridge this knowledge gap and provide insights into EPS adhesion-based applications, this study focuses on evaluating the adhesion performance of EPS from activated sludge on different surfaces. Firstly, EPS were extracted from activated sludge and adjusted to specific total solid (TS) contents and pH levels. The EPS samples were then applied to hydrophilic and hydrophobic surfaces to visualize their interactions behaviours and determine how TS and pH influence adhesion capacity. Secondly, EPS binding capacity was quantified by measuring the amount of fluorescence-labelled microbeads bound to EPS aggregates. Through these investigations, this study aims to assess the feasibility of using EPS from activated sludge as natural adhesives and to explore their potential for broader environmental and industrial applications.

2. Materials and methods

2.1. EPS extraction and characterization

EPS was extracted from activated sludge collected from a wastewater treatment plant in Delft, the Netherlands. The extraction procedure followed the established method described by Felz et al. (2019). Briefly, sludge was heated at 80 °C with 0.5% (w/v) sodium carbonate (Na_2CO_3) for 30 min. Subsequently, the mixture was centrifuged at 3900xg at 4 °C for 20 min. The aqueous supernatant was then adjusted to pH 2.2 by slowly dropping 1.0 M HCl solution, thereby producing stable EPS biopolymer. Afterwards, the samples were centrifuged again under identical conditions, and the EPS biopolymer was eventually collected after discarding acid supernatant. These recovered EPS was stored at 4 °C for subsequent experiments.

In addition, EPS samples from 13 other worldwide wastewater treatment plants were extracted following the same procedure and subjected to identical experiments. The detailed information on the origins and characteristics of these 13 EPS samples can be found in Supporting Information Table S1 and also in the study of De Bruin et al. (2025).

Total solid (TS) and volatile solid (VS) of EPS were measured by drying samples at 105 °C oven for 24 h and at 550 °C oven for 2 h, respectively. EPS were reconstituted in 0.1 M NaOH at a concentration of 1000 mg/L for total sugars and protein quantification. Total sugars were determined using the phenol–sulfuric acid method with glucose as the standard, whereas proteins content was measured via the bicinchoninic acid (BCA) assay with bovine serum albumin (BSA) as the standard. Monosaccharide compositions profile was analysed and quantified by high-performance anion-exchange chromatography with pulsed amperometric detection (HPAEC-PAD). The detailed information on analytical column and monosaccharide standards referred to the previous study (Li et al., 2025).

The particle size distribution of EPS aggregates was measured via a Mastersizer 3000 (Malvern Panalytical, United Kingdom). Circulation between sample chamber and laser compartment was kept constantly to obtain stable size spectra. Peristaltic pump was applied to reduce possibility of the disintegration of EPS aggregates. The zeta potential of EPS was determined using a ζ-potential analyser (Malvern, Zetasizer Nano, ZS90) at room temperature, expressed as millivolts (mV).

A portion of the EPS biopolymer was lyophilized and homogenized for functional group characterization using Fourier Transform Infrared (FT-IR) spectroscopy (Perkin Elmer, Shelton, United States). Spectra were collected in attenuated reflectance (ATR) mode at room temperature. Measurement settings were as follows: a wavenumber range of 4000–600 cm^{-1}, spectral resolution 2 cm^{-1} and 16 acquisitions. The

entire spectra were normalized to the absorbance at 1032 cm^{-1}.

2.2. Adhesion performance of EPS

TS content and pH of EPS influence the structural arrangement of EPS aggregates, thereby altering their adhesion and binding performance. The effects of TS and pH on the adhesive behaviour of EPS were the initial point of this study. The TS content of EPS was adjusted within the range of 0.1–5% (w/v) either by prolonged centrifugation or by dilution with the acid supernatant (to maintain a constant pH). In parallel, the pH of other EPS samples was gradually increased from 2.2 to 11.0 through neutralization with 1.0 M NaOH solution.

For the adhesion experiments, laboratory materials with different surface properties were selected to represent hydrophilic and hydrophobic substrates, i.e., regenerated cellulose dialysis membrane was used as the hydrophilic surface, whereas low-density polyethylene (LDPE) Pasteur pipettes served as the hydrophobic surface. In theory, these materials are made for research use and exhibit exceptional physicochemical stability, maintaining their structural integrity even under extreme conditions. To start the experiment, materials of known surface area were immersed in EPS solutions for 5 min, then removed and placed upright for 2 min to allow unbound EPS to drain off. This procedure was repeated three times to ensure a uniform EPS coating on the surface. Subsequently, the coated materials were soaked in 10 mL of 1.0 M NaOH for 5 min, with occasional vortex to completely detach and dissolve the adhered EPS. The materials were then discarded, and the resulting solution was neutralized with an equal volume of 1.0 M HCl. The total organic carbon (TOC) concentration of the mixture was determined using a Shimadzu TOC-L analyser. The amount of adhered EPS was then calculated from the TOC measurements using a TOC-EPS calibration curve and expressed as mg EPS per square meter of surface area (mg EPS/m^2). Experiments under different conditions were all performed in triplicate tests and each test was conducted with three identical material pieces. The average of these nine pieces was reported as the final adhesion capacity for each condition.

In order to accurately measure the attached EPS on the surface, TOC was employed as an indirect but quantitative indicator of EPS concentration. TOC reflects the total carbon content, representing all carbon-based compounds within EPS. To validate the reliability of TOC as a proxy for EPS quantification, a TOC-EPS correlation was first established. A series of EPS solutions with varying concentrations were prepared in 1.0 M NaOH, then neutralized with 1.0 M HCl and carried on TOC measurement. The resulting calibration curve (Supporting Information, Fig. S2a) exhibited excellent linearity ($R^2 > 0.99$), confirming that TOC is a precise and reliable indicator for quantifying EPS.

2.3. Adsorption studies via isothermal model

To elucidate the mechanisms of EPS attachment to various surfaces, the experimental data were simulated using two widely recognized adsorption isotherm models, Freundlich and Langmuir. The Freundlich model is typically employed to describe heterogeneous multilayer adsorption, whereas the Langmuir model assumes a homogeneous monolayer adsorption process.

The Freundlich isotherm is expressed as follows (Equation (1), and to determine the specific adsorption parameters, the model was transformed into its linear logarithmic form Equation (2).

$$q_e = K_f C^{1/n} \tag{1}$$

$$Inq_e = InK_f + \frac{1}{n} InC \tag{2}$$

Where C represents TS content (%), q_e denotes the quantity of adhered EPS per unit surface area (mg EPS/m^2). The parameters K_f and 1/n characterize the adsorption process, K_f serves as an indicator of adsorption capacity, while 1/n represents adsorption intensity, reflecting both surface heterogeneity and adsorption favorability. The constants K_f and n were derived from the y-intercept and the inverse of the slope, respectively, by plotting lnqe against ln$C$.

Langmuir's isothermal model was calculated using Equation (3), and a linearized double-reciprocal plot Equation (4) was utilized to derive the adsorption parameters.

$$q_e = \frac{q_{max} K_L C_e}{1 + K_L C_e} \tag{3}$$

$$\frac{1}{q_e} = \frac{1}{q_{max} K_L} \bullet \frac{1}{C_e} + \frac{1}{q_{max}} \tag{4}$$

Where q_e and q_{max} denote the equilibrium adsorption amount and the theoretical maximum monolayer adsorption capacity (mg EPS/m^2), respectively. C_e represents the equilibrium concentration of EPS (%) and K_L is the Langmuir constant related to the affinity of the binding sites. By plotting $1/q_e$ over $1/C_e$, the q_{max} and K_L were obtained from the y-intercept and the slope as defined in Equation (4).

2.4. Binding capacity of EPS

In addition to surface adhesion, the interactions between EPS and particulate matters were also investigated. Orange fluorescent polymer microbeads (Cospheric LLC, United States) with a particle size range of 1.5–5.0 μm were used as model particles. The microbeads were first resuspended in ultrapure water to prepare a stock suspension at a concentration of 10 mg/mL. Subsequently, 1.0 mL of the stock solution was mixed with 1.0 mL of EPS solution (3.7% TS) and incubated at room temperature for 10 min under gentle agitation to promote EPS-microbeads interactions.

After 10-minute incubation, the same adhesion procedures described above were applied. Differently, prior to soaking in 0.1 M NaOH, the material surfaces were rinsed three times with ultrapure water to remove unbound or loosely attached microbeads. Thereafter, 0.1 M NaOH was used to dissolve the adhered EPS and release the bound microspheres. The fluorescence intensity of the solution was measured at an excitation wavelength of 606 nm using a spectrophotometer (TECAN Infinite M200 PRO, Männedorf, Switzerland). Microbead quantification was performed using a calibration curve relating fluorescence intensity to microbead concentration (as shown in Supporting Information Fig. S2b), and the results were expressed as microbead mass per gram EPS (mg/mg EPS) and denoted as microbead mass per unit surface area (mg/m^2) as well. The sample in the control group consisting of microbead suspensions without EPS were included in all experiments, to account for potential interference from microbead adhesion to the surface materials.

Commercial sodium alginate (Protaweld RF6650, food grade, FMC BioPolymer) was taken as a reference biopolymer to compare the binding ability of EPS with microbeads. Alginate possesses high intrinsic viscosity and strong gelation kinetics. Preliminary trials indicated that concentrations above 0.5% led to excessive self-crosslinking and the formation of a highly tenacious gel. This made it technically unfeasible to achieve a homogeneous mixture with the microbeads. Therefore, 0.5% was determined as an "operable point" to ensure consistent dispersion and interfacial contact. Given that the same binding capacity tests under identical conditions were performed on alginates with microbeads.

To gain further insight into the mechanisms of EPS interaction with the microspheres, the EPS–microbead mixtures were visualized using fluorescence microscopy equipped with Cy3 filters. For comparison, the morphology of EPS samples without microbeads was also characterized under identical conditions.

3. Results and discussion

3.1. EPS yield and chemical compositions

EPS extracted from activated sludge yielded at 15.6 ± 3.1% of sludge VS. Total sugar and protein contents were 145.8 ± 2.1 mg glucose-equivalent/g VS EPS and 390.5 ± 7.6 mg BSA equivalent/g VS EPS, respectively. Monosaccharides composition profile as listed in Supporting information Table S1 showed that fucose, rhamnose and ribose are the dominant types of sugars while no galactosamine and mannose were detected in extracted EPS.

3.2. Adhesives validation tests on hydrophilic and hydrophobic surfaces

The adhesion abilities of extracted EPS on hydrophilic surfaces were shown in Fig. 1. As shown in Fig. 1a, the amount of adhered EPS initially increased with rising TS content, reaching around 2000 mg/m^2 at low TS levels and peaking at around 6000 mg/m^2 when the TS reached 3.6% TS. However, a further increase in TS to 5.4% resulted in a decrease in adhesion back to 2000 mg/m^2. A strong linear correlation ($R^2 > 0.98$) was observed between adhesion capacity and TS at lower concentrations (< 2%), suggesting that the solid content is one of the key impact factors for EPS adhesion under dilute conditions. In contrast, at higher TS levels the correlation weakened, implying that additional factors, such as changes in the three-dimensional structure of EPS, may affect the adhesion behaviour. These structural alterations likely modify the accessibility of functional sites and consequently affect the overall adhesion performance (Babu et al., 2024; Lee et al., 1994).

Fig. 1b illustrated the adhesion performance of EPS on hydrophilic surfaces as a function of pH at the TS concentration of 2.5%. The amount of adhered EPS peaked of around 3500 mg/m^2 at pH 3.0. Beyond this point, the adhesion capacity declined progressively and stabilized at around 2000 mg/m^2 when the pH exceeded 7.0. This trend suggested that EPS adhesion on hydrophilic surfaces is strongly pH-dependent, with acidic conditions favouring stronger attachment.

Fig. 2 illustrated the adhesion performance of EPS on hydrophobic surfaces. As shown in Fig. 2a, the amount of adhered EPS increased slightly from approximately 1000 mg/m^2 to 2000 mg/m^2 at TS below 2.5%, followed by a sharp increase to over 3000 mg/m^2 at around 4% TS and reaching a maximum of 7000 mg/m^2 at approximately 5.3% TS. In Fig. 2b, the effect of pH on EPS adhesion exhibited a trend similar to that observed on hydrophilic surfaces, except that the highest adhesion was observed at pH 4.0, with a maximum of approximately 3000 mg/m^2, whereas further increases in pH led to a progressive decline in adhesion.

To summarize, both TS and pH are important factors influence EPS adhesion on both hydrophilic and hydrophobic surfaces. Specifically, higher TS generally promoted surface adhesion, while slightly acidic conditions (pH 3.0–4.0) further enhanced the attachment of EPS. However, the adhesion capacity of EPS on hydrophobic surfaces was approximately half of that observed on hydrophilic surfaces under identical conditions, indicating that surface chemistry still played a significant role in modulating EPS-surface interactions.

3.3. Comparison of EPS adhesion on hydrophilic and hydrophobic surfaces

The influence of TS on adhesion capacity (Figs. 1a and 2a) was further evaluated using the Freundlich and Langmuir adsorption isotherm models. These models were employed to characterize the interactions between EPS molecules and both hydrophilic and hydrophobic surfaces. The derived parameters for these simulations are summarized in Table 1. Both models demonstrated a high degree of correlation with the experimental data for the hydrophilic surface ($R^2 > 0.9$). According to Langmuir model, the predicted maximum monolayer adsorption was 3006.2 mg EPS/m^2. This theoretical value aligns with the experimental performance, which exhibited a distinct adsorption plateau at higher TS concentrations; specifically, at TS levels exceeding 1.9%, the adhesion capacity fluctuated around 2500 mg EPS/m^2. These results suggested that EPS adhesion on hydrophilic surfaces primarily followed a monolayer adsorption mechanism, reaching a saturated state at higher TS contents. Consequently, increasing TS content was an effective strategy for enhancing adhesion performance only within the lower concentration range, prior to surface saturation.

In the case of the hydrophobic surface, while both models provided a reasonable fit, a significant discrepancy was observed with the Langmuir prediction. The model predicted a saturated adsorption capacity of 4681.6 mg EPS/m^2. However, experimental observations at higher TS levels, specifically 7248.7 mg/m^2 at 5.3% TS, which far exceeded this theoretical limit. Conversely, the Freundlich model accurately predicted a continuous increase in adhesion, consistent with the experimental trends shown in Fig. 2a. It was hypothesized that once the initial EPS layer was established, it served as a "bridge," facilitating further attachment through polymer entanglement and cohesive interactions rather than simple surface site binding. These findings indicated a high degree of energetic heterogeneity of EPS on the hydrophobic material.

Despite the higher total capacity of the hydrophobic surface, both the Freundlich constant (K_f) and the Langmuir constant (K_L) were higher for the hydrophilic surface. This implied that the hydrophilic surface possesses a higher initial affinity for EPS. While the hydrophilic surface may have a saturated capacity due to its monolayer-limited nature, it "grabs"

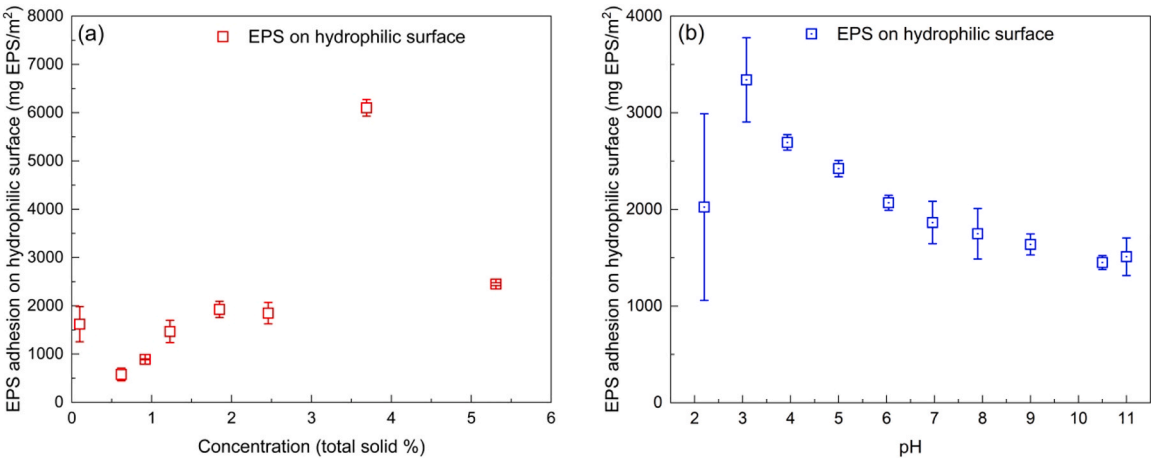

Fig. 1. Quantitative analysis of EPS adhesion on hydrophilic surface (regenerated cellulose membrane) under different conditions. a) Effect of TS content ranging from 0.1% to 5.3% at pH 2.2. b) Effect of pH ranging from 2.2 to 11.0 at TS 2.5%.

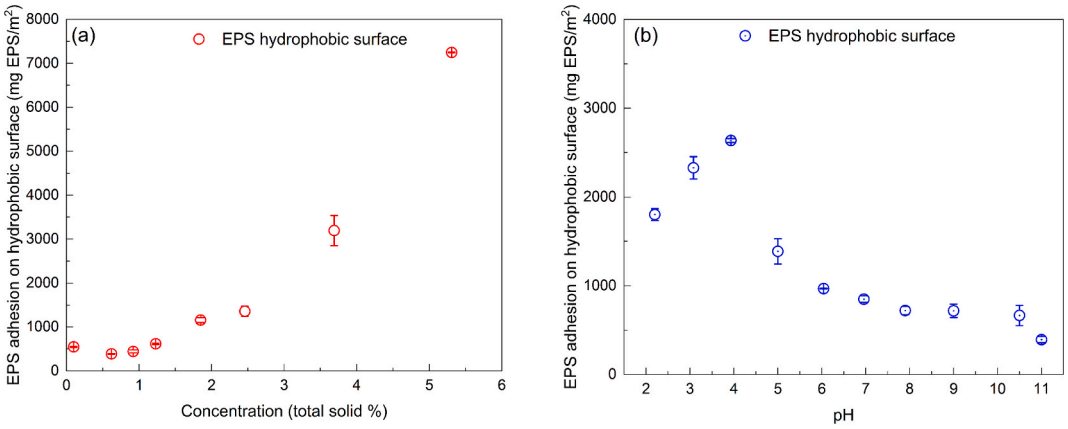

Fig. 2. Quantitative analysis of EPS adhesion on hydrophobic surfaces (low-density polyethylene, LDPE Pasteur pipettes) under different conditions. a) Effect of TS content ranging from 0.1% to 5.3% at pH 2.2. b) Effect of pH ranging from 2.2 to 11.0 at TS 2.5%.

Table 1
Freundlich's and Langmuir's parameters of both hydrophilic and hydrophobic surfaces.

	EPS-Surface	Fitted equation	Correlation coefficient (R^2)	Freundlich constant (K_f, mg EPS/m^2)	Intensity parameter (n)
Freundlich model	EPS-hydrophilic	$\ln q_e = 1.1675\ \ln C + 2.9939$	0.909	986.0	0.86
	EPS-hydrophobic	$\ln q_e = 1.3675\ \ln C + 2.7332$	0.951	553.5	0.84
	EPS-Surface	**Fitted equation**	**Correlation coefficient (R^2)**	**Maximum adsorption (q_{max}, mg EPS/m^2)**	**Langmuir constant (K_L)**
Langmuir model	EPS-hydrophilic	$1/q_e = 0.0094/C_e + 0.00033$	0.931	3006.2	0.035
	EPS-hydrophobic	$1/q_e = 0.0159/C_e + 0.00021$	0.925	4681.6	0.013

EPS molecules significantly more aggressively at low concentrations compared to the hydrophobic surface.

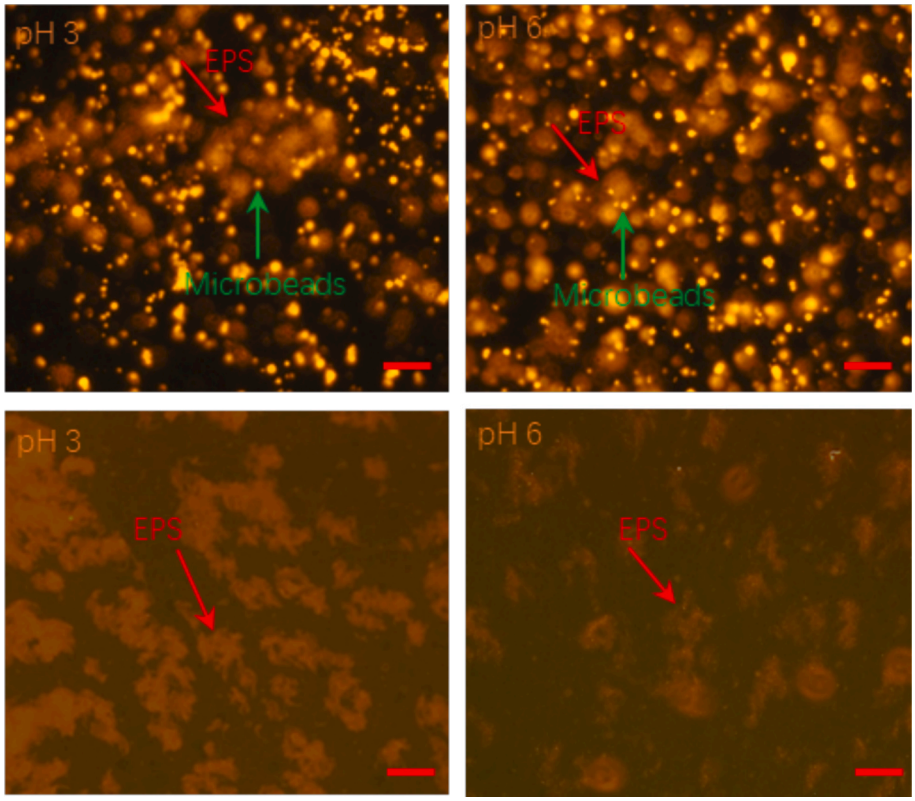

Fig. 3. Fluorescence microscopy images of EPS with (top) and without microbeads (bottom) at pH 3 (left) and pH 6 (right). Microbeads appeared as brighter dots due to fluorescence, while EPS was observed as cloud-like structure due to its autofluorescence. Microbead diameters ranged from 1.5 to 5.0 μm (d_{50} = 1.5–2.0 μm). Scale bar = 20 μm.

3.4. EPS enhanced the attachment of other particles on hydrophilic and hydrophobic surfaces

Based on the adhesion property of EPS on both hydrophilic and hydrophobic surfaces, it was assumed that the EPS may be capable of delivering other particles onto surfaces. Thus, fluorescent microbeads were used as model particles to evaluate the enhancement capacity of EPS. Representative fluorescence microscopy images were shown in Fig. 3, where the small bright dots correspond to microbeads and the cloud-like structures were due to the autofluorescence of EPS. It clearly displayed that most microbeads were in close proximity to EPS, indicating that EPS can effectively bind microbeads on the surface as carriers.

The amount of microbeads bound by per unit EPS was quantified and plotted in Fig. 4a. The results demonstrated considerable binding capacity of exceeding 2.0 mg microbeads per mg EPS. At pH below 5.0, the binding capacity remained relatively constant on both hydrophilic and hydrophobic surfaces. However, at pH values above 5.0, a substantial increase in binding was observed on hydrophobic surfaces, reaching over 4.0 mg microbeads per mg EPS, while the increase on hydrophilic surfaces was modest. This suggested that surface properties can modulate EPS-microbead interactions, resulting in enhancing or competing EPS active groups with microbeads.

Considering that the amount of adhered EPS varied across surfaces, the microbeads load per unit surface area would be a more informative indicator of carrying capacity. Thus the ability of EPS to transport microbeads onto different surfaces were estimated, expressed as mg microbeads per m^2 of surface area. No microbeads remain on the hydrophobic surface in control test without EPS while over 1500 mg beads per m^2 surface area attached achieving by EPS. Regarding hydrophilic surface, there were around 850 mg beads per m^2 surface area on the hydrophilic surface, which was much lower than the samples with EPS assistance (over 4500 mg beads per m^2 surface area). It implied that EPS can enhance the adhesion of microbeads on both surfaces. In addition, as shown in Fig. 4b, the highest loading of microbeads on the hydrophobic surfaces were exhibited at pH 4.0, which decreased slightly at higher pH values. In contrast, microbead attachment on hydrophilic surfaces gradually decreased with increasing pH. These trends closely reflected the changes of EPS adhesion at different pHs, suggesting that the adhesion property of EPS strongly correlated with the enhancement of microbeads adhesion on the surface.

For comparison, commercial sodium alginate was used as a reference. Each milligram of alginate transported 2.9 mg microbeads onto hydrophilic surfaces, which was around 1.5 times higher than EPS (around over 2.0 mg microbeads per mg EPS). No microbead was transferred to hydrophobic surfaces due to the completely hydrophilic nature of alginate. In contrast, EPS exhibited exceptional performance, carrying nearly 6.0 mg microbeads per mg EPS on hydrophobic surface. These results preliminarily demonstrated that EPS can serve as a promising and competitive alternative to other natural binders to enhance the attachment of particles on the surface.

3.5. The adhesion of EPS extracted from global activated sludge samples

Due to the fact the EPS extracted from activated sludge in one WWTP from the Netherlands demonstrated adhesion property on both hydrophobic and hydrophilic surfaces, moreover, this adhesion property made EPS a promising carrier to enhance the attachment of other particles, it is necessary to investigate if EPS recovered from activated sludge collected from worldwide demonstrate the same potential of adhesion on the same surfaces. Thus, another 13 EPS samples recovered from wastewater treatment plants around the world were subjected to the same adhesion tests, and the results were presented in Fig. 5a. Overall, these global EPS samples confirmed the adhesive capability of EPS. On hydrophilic surfaces, the amount of adhered EPS ranged from 1000 to 2500 mg/m^2 at 1.0 g EPS/L and pH 6.0, whereas on hydrophobic surfaces, adhesion ranged from 500 to 1000 mg/m^2, which was lower than the adhesion capacity of EPS on the hydrophilic surfaces. These results confirmed the general capacity of EPS adhering on different surface aligned with that demonstrated by the EPS recovered from one of the WWTP from the Netherlands.

Variations in EPS composition and structure likely contributed to differences in adhesion performance, thus, correlation was searched for from the aspects of total carbohydrates and protein contents as well as sugar monomers (Supporting Information, Table S1)(De Bruin et al., 2025). Pearson correlation analysis with adhesion capacity was performed and shown in Fig. 5b. Protein content exhibited positive influence on both hydrophilic and hydrophobic surfaces adhesion. In contrast, total sugars exhibited negative correlations with adhesion. Among the individual sugars, whereas amino sugars, such as glucosamine, showed relatively weak correlation with adhesion. Ribose and galactose positively contributed to adhesion, whereas fucose, rhamnose, and xylose had inhibitory effects. Galactose and ribose, which contain abundant –OH groups, likely enhanced surface hydrophilicity and EPS swelling, promoting hydrophilic surface adhesion. For hydrophobic surfaces, fucose and rhamnose, with terminal CH_3 groups at the C6 position, were expected to positively affect adhesion while galactose and ribose performed negative influence. However, the observed correlations were opposite, indicating that additional interactions beyond simple sugar compositions, such as glycosidic linkage and structure

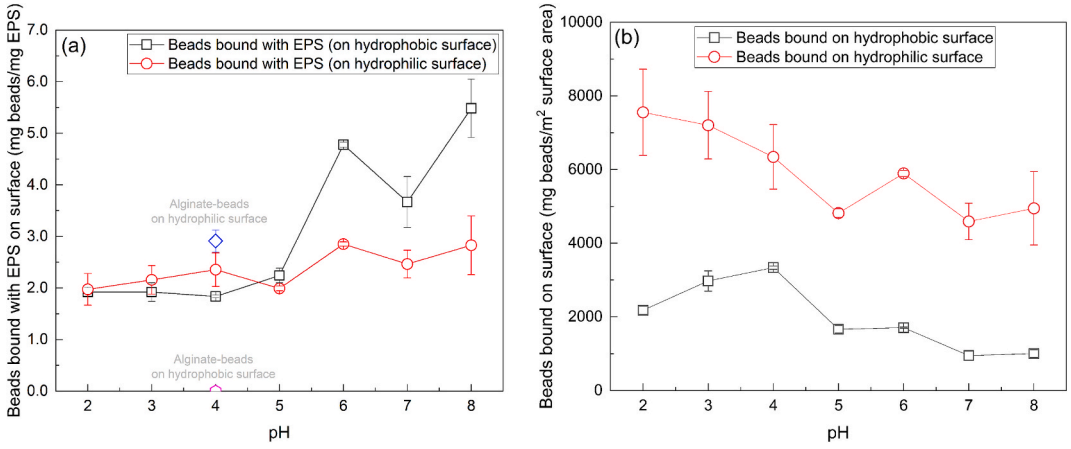

Fig. 4. Quantitative analysis of microbeads bound by EPS onto different surfaces. a) EPS binding capacity at varying pH, expressed as mg microbeads per mg EPS. EPS adhesion amount was taken from the above surface adhesion tests conducted in the absence of microbeads in Fig. 1b and Fig. 2b. Binding capacity of alginate with TS 0.5% at pH 4.0 was scattered as well. b) Microbeads mediated by EPS onto surfaces at different pH, expressed as mg microbeads per m^2 of surface area.

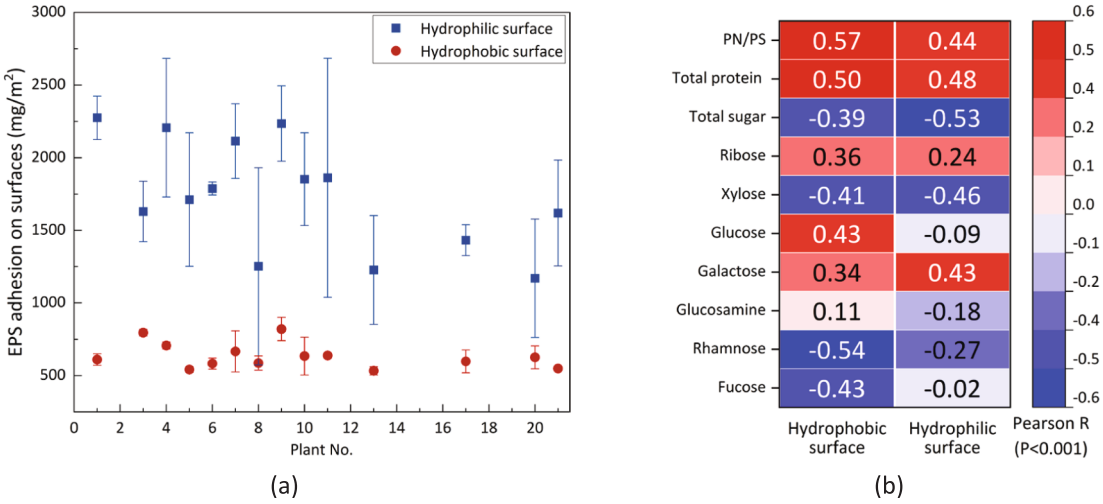

Fig. 5. Adhesion performance of global EPS samples at a concentration of 1.0 g/L and pH 6.0. Plant No. 21 is EPS extracting from Delft sludge. a) Adhesion capacity of EPS on hydrophilic and hydrophobic surfaces. b) Pearson R^2 values from correlation analysis between EPS composition and adhesion performance. Positive and negative R^2 values indicated positive and negative correlations, respectively. Darker colours indicated stronger correlations.

arrangement, could govern EPS adhesion on hydrophobic surfaces.

3.6. Various compositions contributing to EPS adhesion on surfaces

EPS are composed of glycans, proteins, lipids, nucleic acids and so on, with glycans and proteins are dominant (Boleij et al., 2018; Chen et al., 2023; Li et al., 2025; Sen et al., 2025). Correlation analysis of global EPS samples demonstrated that total protein content positively influences adhesion, whereas total sugar content has a negative effect. Sub-units of these compounds like monosaccharides and amino acids crosslinked with each other by various linkages like glycosidic, peptide, and ester bonds (Boleij et al., 2018; Bourven et al., 2015; Li et al., 2025). As revealed by FTIR analysis (Supporting Information, Fig. S3), hydrophilicity-related groups, such as the C═O vibration of amide I, C—N stretch of amide II, and C—O stretch of polysaccharides, and hydrophobicity-related groups, such as the C—H stretch of CH_2 and CH_3 and the C═O of carboxylic acid dimers, exhibited strong signals in EPS samples. With these compounds and structures, EPS possess many charged groups and hydrophobic/hydrophilic moieties. These functional groups played critical roles in determining its physicochemical characteristics and thereby lowered the surface tension of EPS and promoted adhesion performance via hydrogen bonding.

Further analysis of monosaccharide profiles indicated that neutral sugar monomers were strongly associated with adhesion to hydrophilic surfaces, suggesting that interactions derived from these sugars contribute significantly to hydrophilic surface adhesion. In contrast, these sugars had little or unexpected effect on adhesion to hydrophobic surfaces, likely components other than glycans, such as aromatic sites or non-polar regions, contribute to EPS interactions with hydrophobic substrates. Furthermore, ionizable functional groups, including carboxyl, phosphate, amino, and hydroxyl groups, can serve as binding sites for bridging and facilitate adhesion via electrostatic forces (Sen et al., 2025). Phosphodiester groups in nucleic acids have also been shown to mediate EPS binding to polar surfaces (Omoike et al., 2004).

Beyond functional groups, the spatial arrangement and structural organization of EPS can further enhance adhesion through steric effects and polymer chain entanglement. Zaidi et al. (2019) reported that EPS aggregates form through interactions between polysaccharides and proteins, which subsequently adsorb onto other compounds. Even with identical monosaccharide distributions, polysaccharide chain organization can vary in terms of linear versus branched linkages (Boleij et al., 2018; Bourven et al., 2015; Li et al., 2025). Overall, the diverse chemical functional groups, coupled with unique ionization and polymerization properties can affect together to alter the dimensionality of EPS aggregates and confer multifunctionality for interactions with both surfaces and particles. Further investigation is needed to give in-depth explanation on why EPS exhibited higher adhesion on hydrophilic surfaces compared to hydrophobic surfaces.

3.7. Effects of pH and total solids on EPS adhesion

EPS adhesion on surfaces was strongly influenced by both pH and TS, albeit via different mechanisms. EPS solubility is pH-dependent. At low pH, EPS tended to form compact hydrogels with well-defined three-dimensional structures. As the pH increases, the surface charge of EPS aggregates was partially neutralized, leading to loosening of the aggregates and exposure of additional chemical functional groups. Upon contact with surfaces, interactions such as electrostatic forces and hydrogen bonding facilitated EPS binding and altered adhesion behaviour (Ou et al., 2020). At around pH 7, EPS aggregates were partially dissolved under alkaline conditions, resulting in a reduction of particle size from approximately 1000 μm at pH 2.2 to around 100 μm (Supporting Information, Fig. S4). Observations from microscopies also confirmed that EPS aggregates at pH 6 were smaller than those at pH 3. Since the surface was not completely smooth, these smaller EPS molecules would easily block surface crevices and irregularities, then form some thin adhesive layers. This partial coverage of EPS on surface may obstruct further EPS deposition, resulting in reduced overall adhesion. Further increases in pH led to complete dissolution of EPS aggregates, after which resolved EPS morphology remained unchanged with pH change, resulting in relatively constant adhesion capacities between pH 7 and 11.

TS content primarily influenced EPS adhesion by modulating both EPS-surface and inter-EPS aggregate interactions. According to the Langmuir and Freundlich adsorption isotherm models (Table 1), EPS followed a monolayer adsorption pattern on hydrophilic surfaces. Due to the high hydration state of EPS, these monolayers approached saturation gradually as TS increased. This process eventually stabilized the EPS-surface interface, achieving a maximum adhesion capacity. In contrast, model simulations confirmed that EPS adhesion on hydrophobic surfaces occurred through a multilayer adsorption mechanism. Increasing TS content enhanced EPS-EPS cohesive interactions, which effectively outcompeted EPS-water interactions. This shift resulted in the formation of larger aggregates and a reduction in electrostatic repulsion, as evidenced by lower (less negative) zeta potentials (Supporting Information, Table S5). Consequently, additional EPS

molecules were recruited by the initially adhered layer, accumulating on the surface through polymer entanglement. However, because these EPS aggregates preferentially bound to one another rather than forming direct primary bonds with the substrate, these stacked layers exhibited lower mechanical stability and were more susceptible to being rinsed off.

Together, these results indicated that pH governed EPS solubility and exposure of functional groups, while TS controlled inter-aggregate interactions and stacking behaviour. The interplay between these factors determined the overall adhesion of EPS to different surfaces, as well as its capacity to carry microbeads.

3.8. Adhesion and binding properties of EPS

An adhesive is broadly defined as "any substance that is capable of holding or adhering materials together in a functional manner by surface attachment that resists separation". Traditional natural adhesives are typically based on either polysaccharides such as starch-based adhesives (Pascoli Cereda, 2024), protein-based products (Heinritz et al., 2024), or combinations (Han et al., 2023). EPS consisted of various compositions, boosting their potentials as natural adhesives. Global EPS samples from different districts exhibited strong adhesion capacity of EPS on both hydrophilic and hydrophobic surfaces, and they were also capable of carrying large numbers of microbeads, highlighted its potential as a substitute for conventional natural adhesives. The solubility and morphology of EPS were dynamic under such different conditions as changes of pH and TS, enhancing its versatility and resilience for a wide range of applications without any further modifications.

In addition, the comparison of EPS with sodium alginates in this study showed that EPS had the comparative binding capacity with microbeads, i.e. 2.0 mg microbeads of EPS vs. 2.9 mg microbeads of alginates. Furtherly, EPS and alginates were able to transport these bound beads onto hydrophilic surfaces. However, only EPS can deliver these microbeads onto hydrophobic surface while sodium alginate performed no adhesion and thus no microbeads delivery onto hydrophobic surface. At this point, EPS behaved even better performance than alginate which was well-known for its abilities to deliver a wide range of functional ingredients and components (Lee and Mooney, 2012; Yerramathi et al., 2023). In summary, these findings provided solid evidence of EPS could be utilized as biopolymer-based product to act as not only adhesives onto different surfaces but also functional carriers to deliver various targets.

4. Conclusion

This study demonstrated that extracellular polymeric substances (EPS) extracted from excess activated sludge were valuable biopolymers with versatile adhesion and binding properties. Experimental results indicated that lower pH enhances adhesion, reaching capacities of 1000–2500 mg EPS/m^2 on hydrophilic surfaces and 500–1500 mg EPS/m^2 on hydrophobic surfaces. Furthermore, increasing the total solids (TS) content was found to promote adhesion performance. Adsorption isothermal modelling revealed that EPS followed a monolayer adsorption pattern on hydrophilic surfaces, achieving a saturation point of 2500 mg EPS/m^2 at TS levels exceeding 5.3%, while EPS exhibited multilayer adsorption on hydrophobic surfaces via polymer entanglement. Additionally, EPS functioned as an effective binder for particle binding, with a capacity of 2.0–6.0 mg beads per mg EPS, facilitating their transfer onto various surfaces. In summary, these findings confirmed the potential of EPS from activated sludge to function as natural adhesives and binders.

CRediT authorship contribution statement

Ji Li: Writing – review & editing, Writing – original draft, Visualization, Validation, Resources, Methodology, Investigation, Formal analysis, Data curation. **Jeenah Hermelijn:** Methodology, Investigation, Formal analysis. **Mark C.M. van Loosdrecht:** Supervision, Project administration, Funding acquisition. **Yuemei Lin:** Writing – review & editing, Supervision, Methodology, Funding acquisition, Formal analysis, Conceptualization.

Declaration of competing interest

The authors declare that they have no known competing financial interests or personal relationships that could have appeared to influence the work reported in this paper.

Acknowledgement

This research was financially supported by the Novo Nordisk Foundation, Denmark (REThiNk, Grant NNF22OC0071498).

Appendix A. Supplementary data

Supplementary data to this article can be found online at https://doi.org/10.1016/j.biortech.2026.134544.

Data availability

Data will be made available on request.

References

Babu, A., Shams, R., Dash, K.K., Shaikh, A.M., Kovács, B., 2024. Protein-polysaccharide complexes and conjugates: structural modifications and interactions under diverse treatments. J. Agric. Food Res. 18. https://doi.org/10.1016/j.jafr.2024.101510.

Bianchini, A., Bonfiglioli, L., Pellegrini, M., Saccani, C., 2016. Sewage sludge management in Europe: a critical analysis of data quality. Int. J. Environ. Waste Manag. 18 (3).

Boleij, M., Pabst, M., Neu, T.R., Van Loosdrecht, M.C.M., Lin, Y., 2018. Identification of glycoproteins isolated from extracellular polymeric substances of full-scale anammox granular sludge. Environ. Sci. Tech. 52 (22), 13127–13135. https://doi.org/10.1021/acs.est.8b03180.

Bourven, I., Bachellerie, G., Costa, G., Guibaud, G., 2015. Evidence of glycoproteins and sulphated proteoglycan-like presence in extracellular polymeric substance from anaerobic granular sludge. Environ. Technol. (United Kingdom) 36 (19), 2428–2435. https://doi.org/10.1080/09593330.2015.1034186.

Characklis, W.G., Wilderer, P.A.. *Structure and function of biofilms*. https://doi.org/10.1201/9781482284157-7.

Chen, L.M., Erol, Ö., Choi, Y.H., Pronk, M., van Loosdrecht, M., Lin, Y., 2024. The water-soluble fraction of extracellular polymeric substances from a resource recovery demonstration plant: characterization and potential application as an adhesive. Front. Microbiol. 15 (February), 1–8. https://doi.org/10.3389/fmicb.2024.1331120.

Chen, L.M., Keisham, S., Tateno, H., van Ede, J., Pronk, M., van Loosdrecht, M.C.M., Lin, Y., 2023. Alterations of glycan composition in aerobic granular sludge during the adaptation to seawater conditions. ACS ES&T Water. https://doi.org/10.1021/acsestwater.3c00625.

De Bruin, S., Riisgaard-Jensen, M., Hansen, S.H., Van Loosdrecht, M.C.M., Nielsen, P.H., Lin, Y., 2025. Global insights into extracellular polymeric substances from activated sludge: Yield, composition, and microbial communities. Water Res. 124726. https://doi.org/10.1016/j.watres.2025.124726.

Felz, S., Vermeulen, P., van Loosdrecht, M.C.M., Lin, Y.M., 2019. Chemical characterization methods for the analysis of structural extracellular polymeric substances (EPS). Water Res. 157, 201–208. https://doi.org/10.1016/j.watres.2019.03.068.

Flemming, H.C., Wingender, J., 2010. The biofilm matrix. Nat. Rev. Microbiol. 8 (9), 623–633. https://doi.org/10.1038/nrmicro2415.

Flemming, H.C., Wingender, J., Mayer, C., Körstgens, V., Borchard, W., 2010. Cohesiveness in biofilm matrix polymers. In: Community Structure and Co-operation in Biofilms. Cambridge University Press, pp. 87–106. https://doi.org/10.1017/cbo9780511754814.007.

Han, G.Y., Hwang, S.K., Cho, K.H., Kim, H.J., Cho, C.S., 2023. Progress of tissue adhesives based on proteins and synthetic polymers. In Biomaterials Research (Vol. 27, Number 1). BioMed Central Ltd. https://doi.org/10.1186/s40824-023-00397-4.

Harimawan, A., Ting, Y.P., 2016. Investigation of extracellular polymeric substances (EPS) properties of P. aeruginosa and B. subtilis and their role in bacterial adhesion. Colloids Surf. B Biointerfaces 146, 459–467. https://doi.org/10.1016/j.colsurfb.2016.06.039.

Heinritz, C., Ng, X.J., Scheibel, T., 2024. Bio-inspired protein-based and activatable adhesion systems. In Advanced Functional Materials (Vol. 34, Number 35). John Wiley and Sons Inc. https://doi.org/10.1002/adfm.202303609.

Krause, M.J., Bronstein, K.E., 2024. Estimating national sludge generation and disposal from US drinking water and wastewater treatment plants. J. Clean. Prod. 453. https://doi.org/10.1016/j.jclepro.2024.142121.

Lee, J.H., Jung, H.W., Kang, I.-K., Lee, H.B., 1994. Cell behaviour on polymer surfaces with different functional groups. Biomaterials 15 (9), 705–711. https://doi.org/10.1016/0142-9612(94)90169-4.

Lee, K.Y., Mooney, D.J., 2012. Alginate: properties and biomedical applications. In Progress in Polymer Science (Oxford) (Vol. 37, Number 1, pp. 106–126). Elsevier Ltd. https://doi.org/10.1016/j.progpolymsci.2011.06.003.

Li, J., Hao, X., Gan, W., van Loosdrecht, M.C.M., Wu, Y., 2021. Recovery of extracellular biopolymers from conventional activated sludge: potential, characteristics and limitation. Water Res. 205 (July), 117706. https://doi.org/10.1016/j.watres.2021.117706.

Li, J., Hao, X., van Loosdrecht, M.C.M., Lin, Y., 2025. Understanding the ionic hydrogel-forming property of extracellular polymeric substances: differences in lipopolysaccharides between flocculent and granular sludge. Water Res. 268, 122707. https://doi.org/10.1016/j.watres.2024.122707.

Liu, Y., Zhou, J., Lu, S., Ren, J., 2025. Towards the new era of sewage sludge management in China: status, challenges, and perspectives. In Process Safety and Environmental Protection (Vol. 198). Institution of Chemical Engineers. https://doi.org/10.1016/j.psep.2025.107201.

Omoike, A., Chorover, J., Kwon, K.D., Kubicki, J.D., 2004. Adhesion of bacterial exopolymers to α-FeOOH: inner-sphere complexation of phosphodiester groups. Langmuir 20 (25), 11108–11114. https://doi.org/10.1021/la048597.

Ou, Q., Xu, Y., Li, X., He, Q., Liu, C., Zhou, X., Wu, Z., Huang, R., Song, J., Huangfu, X., 2020. Interactions between activated sludge extracellular polymeric substances and model carrier surfaces in WWTPs: a combination of QCM-D AFM and XDLVO prediction. Chemosphere 253. https://doi.org/10.1016/j.chemosphere.2020.126720.

Pascoli Cereda, M., 2024. Starch glues and adhesives. In: Starch Industries: Processes and Innovative Products in Food and Non-Food Uses. Elsevier, pp. 335–348. https://doi.org/10.1016/b978-0-323-90842-9.00009-1.

Sen, S., Tiwari, O.N., Arya, R.K., Bhowmick, T.K., Gayen, K., 2025. New insights on microbial extracellular polysaccharides: production, biological activity, and applications. In Biomass Conversion and Biorefinery. Springer Science and Business Media Deutschland GmbH. https://doi.org/10.1007/s13399-025-06802-3.

Wang, Y., Wang, J., Liu, Z., Huang, X., Fang, F., Guo, J., Yan, P., 2021. Effect of EPS and its forms of aerobic granular sludge on sludge aggregation performance during granulation process based on XDLVO theory. Sci. Total Environ. 795. https://doi.org/10.1016/j.scitotenv.2021.148682.

Yerramathi, B.B., Muniraj, B.A., Kola, M., Konidala, K.K., Arthala, P.K., Sharma, T.S.K., 2023. Alginate biopolymeric structures: versatile carriers for bioactive compounds in functional foods and nutraceutical formulations: a review. In International Journal of Biological Macromolecules (Vol. 253). Elsevier B.V. https://doi.org/10.1016/j.ijbiomac.2023.127067.

Zaidi, N.S., Muda, K., Sillanpää, M., 2019. Effects of extra-cellular polymeric substances towards physical properties of biomass under magnetic field exposure. Int. J. Environ. Sci. Technol. 16 (7), 3801–3808. https://doi.org/10.1007/s13762-018-1897-2.

Zhu, P., Long, G., Ni, J., Tong, M., 2009. Deposition kinetics of extracellular polymeric substances (EPS) on silica in monovalent and divalent salts. Environ. Sci. Tech. 43 (15), 5699–5704. https://doi.org/10.1021/es9003312.